

Cramér-Rao Bound Expressions for Parametric Estimation of Overlapping Peaks: Influence of Prior Knowledge

S. Cavassila,* S. Deval,* C. Huegen,† D. van Ormondt,† and D. Graveron-Demilly*

*Lab. RMN, CNRS UMR 5012, UCB LYON I-CPE, 69622 Villeurbanne, France; and †Applied Physics Department, Delft University of Technology, Delft, The Netherlands

Received July 9, 1999; revised December 13, 1999

We have derived analytical expressions of the Cramér-Rao lower bounds on spectral parameters for singlet, doublet, and triplet peaks in noise. We considered exponential damping (Lorentzian lineshape) and white Gaussian noise. The expressions, valid if a sufficiently large number of samples is used, were derived in the time domain for algebraic convenience. They enable one to judge the precision of any unbiased estimator as a function of the spectral and experimental parameters, which is useful for quantitation objectives and experimental design. The influence of constraints (chemical prior knowledge) on parameters of the peaks of doublets and triplets is demonstrated both analytically and numerically and the inherent benefits for quantitation are shown. Our expressions also enable analysis of spectra comprising many peaks. © 2000 Academic Press

Key Words: MR spectroscopy; quantitation; error estimation; Cramér-Rao bounds; prior knowledge.

1. INTRODUCTION

In signal processing, the Cramér-Rao bound (CRB) (1–3) on the variance of unbiased estimators is widely used as a measure of attainable precision of parameter estimates from a given set of observations (4). This paper enhances its usefulness for magnetic resonance spectroscopy quantitation.

Since clinical conditions do not permit us to obtain standard deviations by repeating measurements, one can use the CRBs instead. Their main properties are as follows:

- The correct model function must be used.
- The precision of the quantitation estimators *cannot* supersede the CRBs.
- The CRBs are independent of the estimation procedure. Consequently, the same CRBs apply to both the frequency and the time domain estimators, provided that they lead to an unbiased estimate.
- The CRBs of the frequencies determine the spectral resolution.
- The CRBs of the amplitudes reveal whether the quantitation is sufficiently precise.
- The CRBs are useful for experimental design, i.e., they allow us to optimize the sample positions (5–7) or, when some

parameter is to be estimated with a specified precision, the minimum number of acquisition averages can be predicted.

- Prior knowledge of relations between model parameters decreases the CRBs and consequently increases the precision.

Consequently, the CRBs give precious insight into the potential performance of quantitation estimators. Evaluation of the CRBs requires inversion of the Fisher information matrix F whose size equals the number of real-valued parameters to be estimated. When a large number of sinusoids is involved, inversion of F becomes analytically intractable, and the CRBs are to be computed numerically. Nevertheless, expressions for CRBs on the frequencies have been reported in a number of papers (8–14) but to the best of our knowledge analytical expressions for all parameters were only given for a singlet or nonoverlapping peaks in Refs. (15–18). We succeeded in deriving *analytical* expressions for CRBs on all free parameters for two and three exponentially damped sinusoids in Gaussian noise, valid if a sufficiently large number of samples is used. These expressions were conveniently derived in the time domain using the symbolic algebra software Maple (19) to invert F . They enable one to judge the precision of model parameters as a function of the spectral and experimental parameters.

First, we rederive the CRBs for a singlet (16) and point out some interesting properties. Then, we treat the cases of a doublet and a triplet with overlapping constituents. Subsequently, we express the influence of overlap on the model parameter estimates of the involved peaks in terms of interaction coefficients. These coefficients provide strong insights concerning the resolving power of the quantitation methods. Then, we study the influence of prior knowledge of relations between model parameters of the constituents of doublet and triplet structures (i.e., knowledge of relative frequencies, amplitude ratios) and point out the inherent benefits on precision. Finally, we show that our theoretical results obtained for two or three peaks can be applied to real-world signals.

2. ANALYTICAL TREATMENT

The CRB theory is based on the so-called Likelihood function (20). Supposing that the noiseless data can be exactly

modeled by the complex-valued time domain model function \hat{x}_n , $n = 0, \dots, N - 1$, the measured data x_n can be written as

$$x_n = \hat{x}_n + b_n, \quad [1]$$

where b_n is Gaussian-distributed noise. Since the noise is complex-valued, the probability of b_n (and sample x_n) is the product of two distribution functions, one for the real part and one for the imaginary part, which are supposedly uncorrelated,

$$P(b_n) = \frac{1}{\sqrt{2\pi\sigma_r^2}} \exp\left(\frac{-b_{nr}^2}{2\sigma_r^2}\right) \frac{1}{\sqrt{2\pi\sigma_i^2}} \exp\left(\frac{-b_{ni}^2}{2\sigma_i^2}\right), \quad [2]$$

where σ_r and σ_i are, respectively, the standard deviations of the real and imaginary parts of the noise. In NMR, generally a quadrature lock-in detection provides the real and imaginary parts of the signal which do not modify the characteristics of the noise distribution. Consequently, we can assume that $\sigma_r = \sigma_i = \sigma$. The joint probability function P of the measurement $x = (x_0, x_1, \dots, x_{N-1})^T$ (the superscript T denotes the transposition), the so-called likelihood function, equals the product of the probability functions of all samples:

$$P(b) = \left(\frac{1}{2\pi\sigma^2}\right)^N \exp\left(-\frac{\sum_{n=0}^{N-1} \|b_n\|^2}{2\sigma^2}\right), \quad [3]$$

where $b = (b_0, b_1, \dots, b_{N-1})^T$.

It is common practice to use the logarithm of this function $P(b)$.

$$L = \ln P(b) = -N \ln 2\pi\sigma^2 - \frac{1}{2\sigma^2} \sum_{n=0}^{N-1} \|b_n\|^2 \quad [4]$$

$$= -N \ln 2\pi\sigma^2 - \frac{1}{2\sigma^2} \sum_{n=0}^{N-1} \times ((x_{nr} - \hat{x}_{nr})^2 + (x_{ni} - \hat{x}_{ni})^2). \quad [5]$$

As can be seen from Eq. [5], in the case of a Gaussian noise, maximizing L amounts to minimizing the sum of squared residues. The Fisher information matrix is defined by (21)

$$F = E \left[\left(\frac{\partial L}{\partial p} \right)^T \left(\frac{\partial L}{\partial p} \right) \right], \quad [6]$$

where E stands for Expectation value and $p = (p_1, p_2, \dots, p_{N_p})^T$ represents the N_p real-valued model parameters. Working out the expectation, F can be expressed as the real part of a complex-valued matrix product (22), i.e.,

$$F = \frac{1}{\sigma^2} \Re(D^H D), \quad [7]$$

where $D_{nl} = \partial \hat{x}_n / \partial p_l$ for $n = 0, 1, \dots, N - 1$ and $l = 1, 2, \dots, N_p$. The size of F equals the number N_p of real-valued parameters to be estimated. The superscript H denotes Hermitian conjugation and \Re stands for real part. The matrix D requires computation of the derivatives of the samples \hat{x}_n with respect to the parameters p_l using their true values. The CRBs on the standard deviations of the estimated parameters p_l are given by the fundamental Cramér-Rao inequality,

$$\sigma_{p_l} \geq \text{CRB}_{p_l} = \sqrt{(F^{-1})_{ll}}. \quad [8]$$

As seen from Eq. [8], evaluation of the CRBs requires inverting the Fisher information matrix F .

If we suppose that the signal can be modeled by a sum of K exponentially damped sinusoids, each model sample \hat{x}_n can be written as

$$\begin{aligned} \hat{x}_n &= \sum_{k=1}^K c_k \exp((\alpha_k + j\omega_k)nt_s) \exp(j\phi_k) \\ &\equiv \sum_{k=1}^K c_k z_k^n \exp(j\phi_k), \quad n = 0, 1, \dots, N - 1, \end{aligned} \quad [9]$$

where c , $\alpha = -1/T_2^*$, ω and ϕ are, respectively, the amplitudes, the damping factors (minus the inverse of the apparent transverse relaxation time T_2^*), the angular frequencies, and the phases, $j^2 = -1$, t_s is the sampling interval, and the z_k are the poles of the signal. With this model function the elements of F contain summations of the form

$$\sum_{n=0}^{N-1} (nt_s)^i \exp((\alpha + j\omega)nt_s), \quad [10]$$

where i equals 0, 1, or 2. In order to make later calculations tractable, the following simplifications were adopted. First, $t_N = Nt_s$ was assumed large enough to make the functions $t^i \exp((\alpha + j\omega)t)$, $i = 0, 1, 2$, small with respect to the noise level. This leads to asymptotic expressions of the CRBs (15). Second, considering that the sampling rate t_s^{-1} is satisfied and t_N is large (23), Eq. [10] can be approximated by analytical integral expressions given in (24),

$$\int_0^\infty t^i \exp((\alpha + j\omega)t) dt = -i!(\alpha + j\omega)^{-i-1}, \quad \alpha < 0. \quad [11]$$

With the model function in Eq. [9], the size of F equals $4K$. Then, when a large number of sinusoids is involved, analytical inversion of matrix F becomes intractable and the CRBs must be computed numerically rather than analytically. Nevertheless, if prior knowledge on relations between model parameters is available, constraints can be imposed on model parameters, which in turn reduces the size of F .

We have succeeded in deriving analytical expressions of the CRBs on spectral parameters for isolated (well separated) peaks and for two and three overlapping peaks. These expressions enable one to make an estimation of the precision of parameters as a function of spectral and acquisition parameters. Consequently, they are useful for experimental design. Moreover, they obviate the need for running extensive numerical calculations.

3. THE CRAMÉR-RAO LOWER BOUNDS FOR ISOLATED AND OVERLAPPING PEAKS

Singlets or Isolated Peaks

For a single or isolated peak, characterized by four parameters $p = (c, \alpha, \phi, \omega)^T$, F^{-1} is the following 4×4 matrix (15, 16):

$$F^{-1} = -t_s \sigma^2 \begin{pmatrix} c & \alpha & \phi & \omega \\ 4\alpha & 4\alpha^2/c & 0 & 0 \\ 4\alpha^2/c & 8\alpha^3/c^2 & 0 & 0 \\ 0 & 0 & 4\alpha/c^2 & 4\alpha^2/c^2 \\ 0 & 0 & 4\alpha^2/c^2 & 8\alpha^3/c^2 \end{pmatrix}. \quad [12]$$

Recall that this result is valid if the number N of samples is sufficiently large implying that $t_N^i \exp((\alpha + j\omega)t_N)$, $i = 0, 1, 2$, is small.

The diagonal elements of F^{-1} are the variance bounds on the parameters (squares of the CRBs). The nondiagonal elements of F^{-1} are the covariance bounds between the model parameters and the correlation between model parameters p_i and p_m is governed by the relation

$$\rho_{lm} = \frac{(F^{-1})_{lm}}{\sqrt{(F^{-1})_{ll}(F^{-1})_{mm}}}. \quad [13]$$

From Eq. [12] one can infer the following:

- The CRBs on the angular frequency and the damping are equal to each other. They depend strongly on the damping and are inversely proportional to the signal-to-noise ratio (SNR). The expression is

$$\text{CRB}_\omega = \text{CRB}_\alpha = 2\sqrt{2}(-\alpha)^{3/2}\sqrt{t_s}\frac{\sigma}{c}. \quad [14]$$

- The CRB on the amplitude depends only on the noise and *not* on the amplitude. It is c times that on the phase. The expression is

$$\text{CRB}_c = c \text{CRB}_\phi = 2(-\alpha)^{1/2}\sqrt{t_s}\sigma. \quad [15]$$

- Using Eqs. [12] and [13] one finds that both the correlation between the angular frequency and phase and the correlation between the damping and the amplitude equal $1/\sqrt{2}$. All other correlations are zero.

- All CRBs are proportional to the square root of the sampling interval. This suggests that oversampling decreases the CRBs. However, the noise obtained after the antialiasing low-pass filter included in the receiver chain is still, white, and Gaussian and its spectral density is constant, consequently $\sigma/\sqrt{\Delta F} = \sigma\sqrt{t_s} = c^{\text{st}}$ where ΔF is the spectral bandwidth (25). Consequently, no gain should be expected but note that the reduction of the quantitation noise due to oversampling (26) is not taken into account.

The noise standard deviation σ is inversely proportional to the square root of the number of acquisition averages. Thus, when some parameter is to be estimated with a specified precision, the minimum number of acquisition averages can be predicted.

The above results are also valid for a singlet peak that is isolated from the other peaks in the spectrum (see next section).

Doublets

For two overlapping peaks with parameters $c_1, \omega_1, \alpha_1, \phi_1; c_2, \omega_2 = \omega_1 + \Delta\omega, \alpha_2, \phi_2$ ($\Delta\omega = 2\pi J$, J being the scalar coupling) and using Eq. [11], we derived analytical expressions for the 64 elements of F (see Table 1). To simplify the expressions and remove the dependency in ϕ , we assumed that ϕ_1 and ϕ_2 are equal (e.g., when the receiver dead time is equal to 0 or known). We introduced the overlap factor R ,

$$R = \frac{\alpha_1 + \alpha_2}{\Delta\omega}, \quad [16]$$

which characterizes the doublet shape.

In the case of well-separated peaks, the nondiagonal elements of F connecting the 4×4 diagonal blocks are small ($R \rightarrow 0$) and the matrix approaches a block diagonal matrix; see Fig. 1. The matrix expressions given in Eq. [12] can be easily derived by inverting each 4×4 diagonal block separately. In the case of overlapping peaks, the elements connecting the 4×4 diagonal blocks are significant which in turn implies that one must analytically invert the entire 8×8 matrix F . For that, we used Maple and arrived at interesting analytical expressions for F^{-1} (27).

For both peaks, the CRBs on the angular frequencies and dampings turn out to be equal to each other:

TABLE 1
Fisher Matrix for Two Overlapping Peaks Assuming That $\phi_1 = \phi_2$

c_1	α_1	ϕ_1	ω_1	c_2	α_2	ϕ_2	ω_2
$-\frac{1}{2\alpha_1}$	$\frac{c_1}{4\alpha_1^2}$	0	0	$-\frac{R^2}{(\alpha_1 + \alpha_2)(1 + R^2)}$	$-\frac{c_2 R^2(1 - R^2)}{(\alpha_1 + \alpha_2)^2(1 + R^2)^2}$	$-\frac{c_2 R}{(\alpha_1 + \alpha_2)(1 + R^2)}$	$2\frac{c_2 R^3}{(\alpha_1 + \alpha_2)^2(1 + R^2)^2}$
$\frac{c_1}{4\alpha_1^2}$	$-\frac{c_1^2}{4\alpha_1^3}$	0	0	$-\frac{c_1 R^2(1 - R^2)}{(\alpha_1 + \alpha_2)^2(1 + R^2)^2}$	$2\frac{c_1 c_2 R^4(3 - R^2)}{(\alpha_1 + \alpha_2)^3(1 + R^2)^3}$	$2\frac{c_1 c_2 R^3}{(\alpha_1 + \alpha_2)^2(1 + R^2)^2}$	$2\frac{c_1 c_2 R^3(1 - 3R^2)}{(\alpha_1 + \alpha_2)^3(1 + R^2)^3}$
0	0	$-\frac{c_1^2}{2\alpha_1}$	$\frac{c_1^2}{4\alpha_1^2}$	$\frac{c_1 R}{(\alpha_1 + \alpha_2)(1 + R^2)}$	$-\frac{c_1 c_2 R^3}{2(\alpha_1 + \alpha_2)^2(1 + R^2)^2}$	$-\frac{c_1 c_2 R^2}{(\alpha_1 + \alpha_2)(1 + R^2)}$	$-\frac{c_1 c_2 R^2(1 - R^2)}{(\alpha_1 + \alpha_2)^2(1 + R^2)^2}$
0	0	$\frac{c_1^2}{4\alpha_1^2}$	$-\frac{c_1^3}{4\alpha_1^3}$	$-\frac{c_1 R^3}{(\alpha_1 + \alpha_2)^2(1 + R^2)^2}$	$2\frac{c_1 c_2 R^4(1 - 3R^2)}{(\alpha_1 + \alpha_2)^3(1 + R^2)^3}$	$-\frac{c_1 c_2 R^2(1 - R^2)}{(\alpha_1 + \alpha_2)^2(1 + R^2)^2}$	$2\frac{c_1 c_2 R^4(3 - R^2)}{(\alpha_1 + \alpha_2)^3(1 + R^2)^3}$
$\frac{R^2}{(\alpha_1 + \alpha_2)(1 + R^2)}$	$-\frac{c_1 R^2(1 - R^2)}{(\alpha_1 + \alpha_2)^2(1 + R^2)^2}$	$\frac{c_1 R}{(\alpha_1 + \alpha_2)(1 + R^2)}$	$-\frac{c_1 R^3}{2(\alpha_1 + \alpha_2)^2(1 + R^2)^2}$	$-\frac{1}{2\alpha_2}$	$\frac{c_2}{4\alpha_2^2}$	0	0
$-\frac{c_2 R^2(1 - R^2)}{(\alpha_1 + \alpha_2)^2(1 + R^2)^2}$	$2\frac{c_1 c_2 R^4(3 - R^2)}{(\alpha_1 + \alpha_2)^3(1 + R^2)^3}$	$-\frac{c_1 c_2 R^3}{2(\alpha_1 + \alpha_2)^2(1 + R^2)^2}$	$-\frac{c_1 c_2 R^3(1 - 3R^2)}{2(\alpha_1 + \alpha_2)^3(1 + R^2)^3}$	$\frac{c_2}{4\alpha_2^2}$	$-\frac{c_2^2}{4\alpha_2^3}$	0	0
$-\frac{c_2 R}{(\alpha_1 + \alpha_2)(1 + R^2)}$	$2\frac{c_1 c_2 R^3}{(\alpha_1 + \alpha_2)^2(1 + R^2)^2}$	$-\frac{c_1 c_2 R^2}{(\alpha_1 + \alpha_2)(1 + R^2)}$	$-\frac{c_1 c_2 R^2(1 - R^2)}{(\alpha_1 + \alpha_2)^2(1 + R^2)^2}$	0	0	$-\frac{c_2^2}{2\alpha_2}$	$\frac{c_2^2}{4\alpha_2^2}$
$2\frac{c_2 R^3}{(\alpha_1 + \alpha_2)^2(1 + R^2)^2}$	$2\frac{c_1 c_2 R^4(1 - 3R^2)}{(\alpha_1 + \alpha_2)^3(1 + R^2)^3}$	$-\frac{c_1 c_2 R^2(1 - R^2)}{(\alpha_1 + \alpha_2)^2(1 + R^2)^2}$	$2\frac{c_1 c_2 R^4(3 - R^2)}{(\alpha_1 + \alpha_2)^3(1 + R^2)^3}$	0	0	$\frac{c_2^2}{4\alpha_2^2}$	$-\frac{c_2^2}{4\alpha_2^3}$

$F = \frac{1}{I_0 \sigma^2}$

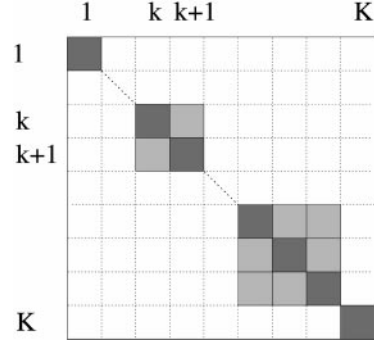


FIG. 1. Example of a block diagonal Fisher information matrix F for a signal containing K peaks. Each square represents a 4×4 block. The elements in the white squares are near zero.

$$\text{CRB}_{\omega_k} = \text{CRB}_{\alpha_k} = \text{corr}_{\omega} \text{CRB}_{\omega_k}^s, \quad k = 1, 2, \quad [17]$$

where $\text{CRB}_{\omega_k}^s$ is defined by Eq. [14] and pertains to peak k considered isolated (the superscript s indicates the case of a single peak). Furthermore,

$$\text{corr}_{\omega} = \frac{1 + R^2}{1 + R^2 \eta^2} \geq 1, \quad [18]$$

where

$$\eta = \frac{\alpha_1 - \alpha_2}{\alpha_1 + \alpha_2} \quad [19]$$

represents an asymmetry factor of the doublet. Equation [17] is seen to be the product of the CRB pertaining to an isolated peak and a term corr_{ω} denoting the interaction between the two peaks. The term corr_{ω} depends on the dampings and on the frequency separation of the two peaks but *not* on their amplitudes. In addition, Eq. [18] shows that the interaction between two signal components is small when one decays much more slowly than the other ($|\alpha_2| \ll |\alpha_1|$) or when the peaks are well separated such that $R \rightarrow 0$. Figure 2a displays corr_{ω} as a function of the inverse of the normalized parameters $\alpha_1' = \alpha_1/\Delta\omega$ and $\alpha_2' = \alpha_2/\Delta\omega$. Note that corr_{ω} is largest when the two dampings are equal.

The CRB on the amplitude c_k is c_k times that on the phase ϕ_k . As before, the expression is the product of the CRB of a single peak and an interaction term

$$\text{CRB}_{c_k} = c_k \text{CRB}_{\phi_k} = \text{corr}_{c_k} \text{CRB}_{c_k}^s, \quad k = 1, 2, \quad [20]$$

where $\text{CRB}_{c_k}^s$ is defined by Eq. [15] and pertains to the peak k considered isolated and

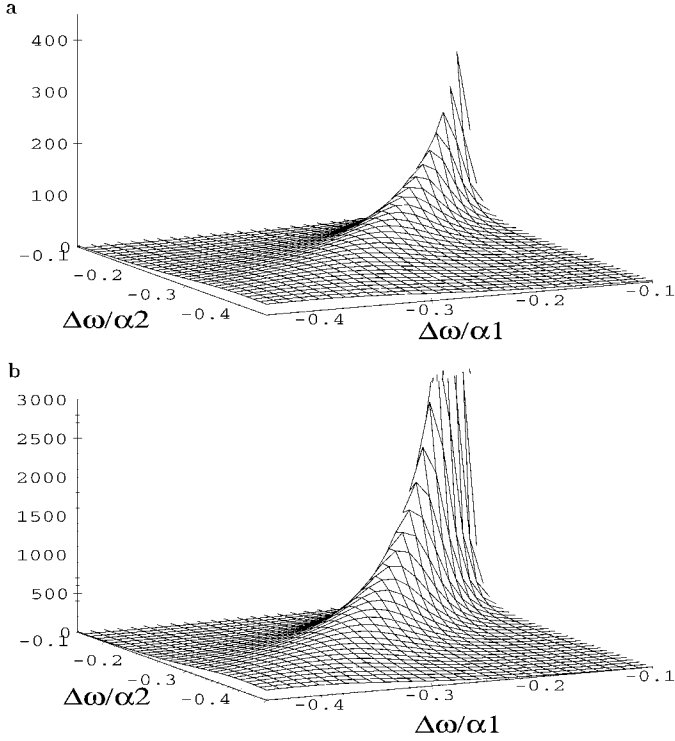


FIG. 2. 3D maps showing the interaction factors for a doublet. (a) corr_ω and (b) corr_{c_1} as a function of the normalized parameters $\Delta\omega/\alpha_1$ and $\Delta\omega/\alpha_2$.

$$\text{corr}_{c_1} = \sqrt{\frac{(1+R^2)[(1+R^2)^2 + 4\alpha'_1\alpha'_2(1+\alpha'^2_2 - 3\alpha'^2_1 + 6\alpha'_1\alpha'_2)]}{(1+R^2\eta^2)^3}}. \quad [21]$$

The quantity corr_{c_2} is obtained by exchanging the subscripts 1 and 2 in the expression of corr_{c_1} . Note that $\text{corr}_{c_1} = \text{corr}_{c_2}$ when $\alpha_1 = \alpha_2$. The interaction term corr_{c_k} and consequently CRB_{c_k} does *not* depend on the amplitudes of the two peaks but *only* on the overlap which in turn is governed by R , defined in

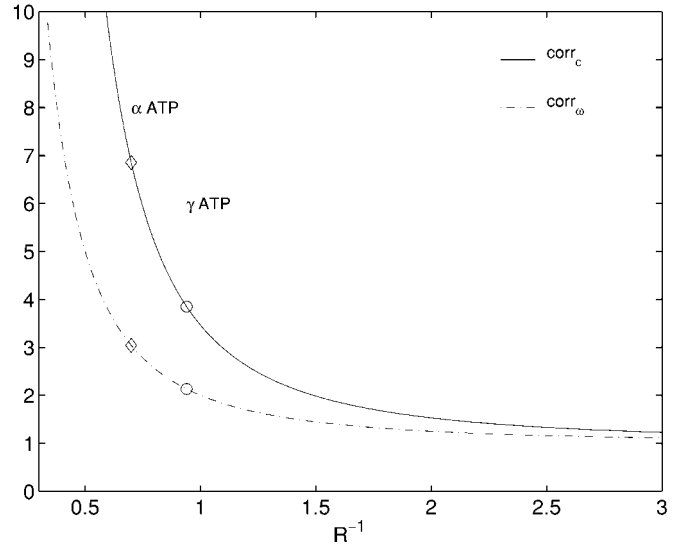


FIG. 3. Interaction terms corr_c and corr_ω for a symmetric doublet as a function of the absolute value of the inverse of the overlap factor R . The marks correspond to the estimated absolute R^{-1} values of ATP multiplets.

Eq. [16]. Consequently, statistically speaking no problems are to be expected when one peak of the spectrum is very strong such as the water or fat peaks. This result suggests that prior subtraction of a dominant signal is not necessary, provided that its model function is known. Moreover, one can infer that a broad overlapping background peak severely hampers the precise determination of the parameters of a superimposed peak of interest.

Figure 2b shows the interaction term corr_{c_1} as a function of the inverse of α'_1 and α'_2 . Like corr_ω , corr_{c_1} is maximal when the two dampings are equal and can reach very large values. Equations [18] and [21] are simpler in the case of a symmetric doublet with parameters $\alpha = \alpha_1 = \alpha_2$, $c = c_1 = c_2$, $\phi = \phi_1 = \phi_2$, $\omega_2 = \omega_1 + \Delta\omega$, and $R = (2\alpha)/\Delta\omega$. The corresponding CRB expressions are given in Table 2. The interaction terms corr_c and corr_ω are displayed in Fig. 3 as a

TABLE 2

Cramer-Rao Lower Bounds on the Parameters of a Symmetric Doublet as a Function of the Overlap Factor $R = (2\alpha)/\Delta\omega$ and of the CRBs on the Isolated-Peak Parameters $\text{CRB}_c^s = 2(-\alpha)^{1/2}\sqrt{t_s}\sigma/c$ and $\text{CRB}_\omega^s = 2\sqrt{2}(-\alpha)^{3/2}\sqrt{t_s}\sigma/c$, (a) No Prior Knowledge, (b) Fixed Frequencies, (c) Fixed Frequencies and Dampings, and (d) Chemical Prior Knowledge as Defined in the Text

	$\text{CRB}_{\omega_1} = \text{CRB}_{\omega_2}$	$\text{CRB}_{c_1} = \text{CRB}_{c_2}$
a	$(1+R^2) \text{CRB}_\omega^s$	$\frac{\sqrt{(1+2R^2)(1+R^2)}}{(1+5R^2+13R^4+25R^6)} \text{CRB}_c^s$
b	0	$\frac{1}{\sqrt{2}}\sqrt{1+R^2} \text{CRB}_c^s$
c	0	$\frac{\sqrt{(1+R^2)(1+3R^2+2R^6)}}{\sqrt{2(1+8R^2+7R^4+4R^8)}} \text{CRB}_c^s$
d	$\sqrt{\frac{(1+R^2)^3(1+2R^2)}{2(1+8R^2+7R^4+4R^8)}} \text{CRB}_\omega^s$	$\frac{\sqrt{(1+2R^2)(1+R^2)}}{\sqrt{2(1+8R^2+7R^4+4R^8)}} \text{CRB}_c^s$

TABLE 3

Cramer-Rao Lower Bounds on Symmetric Triplet Parameters as a Function of the Overlap Factor $R = (2\alpha)/\Delta\omega$ and of the CRBs on the Parameters of the Central Peak Considered Isolated ($\text{CRB}_c^s = 2(-\alpha)^{1/2}\sqrt{\tilde{I}_s}\sigma$ and $\text{CRB}_\omega^s = 2\sqrt{2}(-\alpha)^{3/2}\sqrt{\tilde{I}_s}\sigma/c$), (a) No Prior Knowledge, (b) Fixed Frequencies, (c) Fixed Frequencies and Dampings, and (d) Chemical Prior Knowledge as Defined in the Text

$\text{CRB}_{\omega_i} \quad i = 1, 2, 3$	
a	$\text{CRB}_{\omega_1} = \text{CRB}_{\omega_3} = 0.25(1 + R^2)(4 + R^2) \text{CRB}_\omega^s$ $\text{CRB}_{\omega_2} = 0.5(1 + R^2)^2 \text{CRB}_\omega^s$
b	$\text{CRB}_{\omega_1} = \text{CRB}_{\omega_2} = \text{CRB}_{\omega_3} = 0$
c	$\text{CRB}_{\omega_1} = \text{CRB}_{\omega_2} = \text{CRB}_{\omega_3} = 0$
d	$\text{CRB}_{\omega_1} = \text{CRB}_{\omega_2} = \text{CRB}_{\omega_3} = \sqrt{\frac{(3 + 8R^2 + 2R^4)(1 + R^2)^3(4 + R^2)^3}{8(144 + 1536R^2 + 2555R^4 + 1204R^6 + 825R^8 + 672R^{10} + 256R^{12} + 48R^{14} + 4R^{16})}} \text{CRB}_\omega^s$
$\text{CRB}_{c_i} \quad i = 1, 2, 3$	
a	$\text{CRB}_{c_1} = \text{CRB}_{c_3} = 0.125\sqrt{2(32 + 160R^2 + 298R^4 + 241R^6 + 80R^8 + 9R^{10})} \text{CRB}_c^s$ $\text{CRB}_{c_2} = \sqrt{1 + 8R^2 + 26R^4 + 32R^6 + 13R^8} \text{CRB}_c^s$
b	$\text{CRB}_{c_1} = \text{CRB}_{c_3} = \sqrt{\frac{256 + 1920R^2 + 5664R^4 + 9272R^6 + 5001R^8 + 12108R^{10} + 12157R^{12} + 5610R^{14}}{8(32 + 160R^2 - 166R^4 + 509R^6 - 434R^8 + 221R^{10})}} \text{CRB}_c^s$ $\text{CRB}_{c_2} = \sqrt{\frac{(1 + R^2)^2(4 + 29R^2 + 82R^4 + 165R^6)}{(4 + 21R^2 - 24R^4 + 13R^6)}} \text{CRB}_c^s$
c	$\text{CRB}_{c_1} = \text{CRB}_{c_3} = \sqrt{\frac{(1 + R^2)(4 + R^2)}{8}} \text{CRB}_c^s$ $\text{CRB}_{c_2} = \frac{1}{\sqrt{2}}(1 + R^2) \text{CRB}_c^s$
d	$\text{CRB}_{c_1} = \text{CRB}_{c_3} = \sqrt{\frac{(96 + 360R^2 + 132R^4 + 190R^6 + 138R^8 + 36R^{10} + 4R^{12})(1 + R^2)(4 + R^2)}{1280 + 13184R^2 + 22560R^4 + 12608R^6 + 8771R^8 + 6582R^{10} + 2439R^{12} + 444R^{14} + 36R^{16}}} \text{CRB}_c^s$ $\text{CRB}_{c_2} = 2 \text{CRB}_{c_1} = 2 \text{CRB}_{c_3}$

function of R^{-1} . Of course, if the two peaks strongly overlap ($R \rightarrow \infty$) they reach large values ($\text{corr}_c \rightarrow \infty$ and $\text{corr}_\omega \rightarrow \infty$). Note that for $R = 2$, for example, corr_ω is around 5 and that corr_c is as large as 15 revealing quantitation difficulties.

Summarizing, we have for doublets the following:

- The CRBs for a peak of a doublet equal the product of the CRB of the peak considered isolated times a term “corr” that represents the interaction between the two peaks of the doublet. This provides quick insight into the effect of overlap.
- The interaction terms corr_ω and corr_α do not depend on the amplitudes c_k . In addition, they do not depend on which peak of the doublet is considered.
- The interaction terms corr_c are also independent of the amplitudes. On the other hand, they do depend on which peak of the doublet is considered.

Triplets

In general, a triplet entails a Fisher matrix of size 12×12 . To make analytical inversion of such a matrix tractable, we assumed that the triplet was symmetric, $\alpha = \alpha_1 = \alpha_2 = \alpha_3$, $c = c_1 = c_3 = \frac{1}{2}c_2$, $\phi = \phi_1 = \phi_2 = \phi_3$, $\omega_3 = \omega_1 + 2\Delta\omega = \omega_2 + \Delta\omega$. Using the same approximations as before, we calculated the 144 elements of F . Inverting F with Maple, we obtained the CRB expressions in Table 3. The expressions are

more complicated than those for doublets, but the properties of the latter remain valid for triplets. Additional properties are as follows:

- The interaction terms corr_ω and corr_α depend on which peak of the triplet is considered. However, for strong overlap, the dominating power of R becomes 4 for all peaks of the triplet.
- The interaction terms corr_c depend on which peak of the triplet is considered. For strong overlap, the dominating power of R becomes 5 for the outer peaks but 4 for the central peak. Quantitation of the latter then becomes progressively more precise than that of the former.

4. INFLUENCE OF PRIOR KNOWLEDGE

Methods based on nonlinear least-squares fitting such as VARPRO (22, 28, 29) or AMARES (30) and some recent SVD-based methods allow us to include prior knowledge of the poles (31, 32), the frequencies (33), and the phases (34). Incorporation of prior knowledge in turn reduces the number of free parameters and consequently the size of the information matrix F . Note that prior knowledge is not always trustworthy in *in vivo* studies. For example, the resonance frequency of a metabolite may depend on pH, and additional unknown com-

ponents may be superimposed on multiplets. As mentioned in the Introduction, the correct model function must be used which implies that the prior information be correct. If we now assume linear relations between model parameters of the same kind (for example, $c_l = ac_m$ and $\omega_l = \omega_m + b$, in which a and b are real-valued constants), we introduce the *prior knowledge* matrix P ,

$$P_{lm} = \begin{pmatrix} \frac{\partial p_l}{\partial p'_m} \end{pmatrix}, \quad l = 1, 2, \dots, 4K, \quad m = 1, 2, \dots, L. \quad [22]$$

F can then be expressed as

$$F = \frac{1}{\sigma^2} \Re(P^T D^H D P), \quad [23]$$

where $p' = (p'_1, \dots, p'_L)^T$ corresponds to the L ($L \leq 4K$) unconstrained parameters p_l to be estimated, and D has been defined previously. When $L = 4K$, P is the identity matrix. The ensuing CRBs are given in Eq. [8].

This new formulation of the Fisher matrix (Eq. [23]) allows imposition of linear relations between model parameters in a simple manner. We have derived analytical expressions CRB_{pk} for symmetric doublets, triplets, and three sets of prior knowledge which successively involve an increasing number of constraints: (1) fixed frequencies; (2) fixed frequencies and dampings; (3) chemical prior knowledge on multiplet structures, namely (i) weak, fixed scalar couplings, and amplitude ratio of 1:1 for a doublet and 1:2:1 for a triplet, (ii) equal dampings, and (iii) equal phases (not too restrictive for close peaks and small dead time). The results are presented, respectively, in Tables 2 and 3 for symmetric doublets and triplets. The CRB_{pk} expressions are generally more complicated than those obtained without prior knowledge. But they are still equal to the product of the CRB of the peak considered isolated times an interaction term.

The ratio $\text{CRB}_{pk}/\text{CRB} < 1$ provides immediate insight into the benefit of prior knowledge on parameter precision. The inverse of this ratio is displayed in Fig. 4 as a function of R^{-1} for the amplitudes of symmetric doublets and triplets. The linear relations bring about a reduction of the CRBs. We find that a reduction of errors can occur even for weak overlap ($R \rightarrow 0$). For example, when the poles are fixed, the ratio $\text{CRB}_{pk}/\text{CRB} \rightarrow 1/\sqrt{2}$ for both doublets and triplets. When imposing the mentioned chemical prior knowledge, $\text{CRB}_{pk}/\text{CRB} \rightarrow 1/\sqrt{2}$ for doublets. Whenever the peaks involved overlap, i.e., when the dampings are large or the frequencies close ($R \rightarrow \infty$), the error reduction can be by an *order of magnitude*. This is more pronounced for triplets than for doublets. In most cases, the largest reduction results from the chemical prior knowledge mentioned above. Hence, its imposition is highly recommendable.

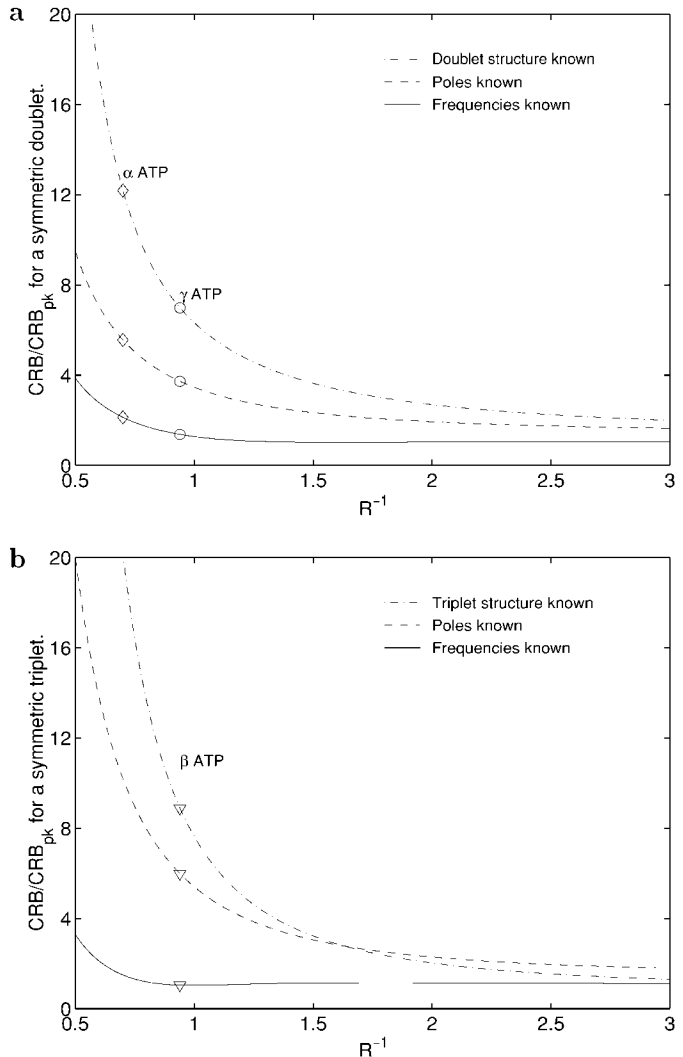


FIG. 4. Inverse reduction factors of the errors on (a) amplitudes of a symmetric doublet and (b) amplitude of the central peak of a symmetric triplet, as a function of the absolute value of the inverse of the overlap factor R . Three sets of prior knowledge were imposed: (1) fixed frequencies (solid line); (2) fixed frequencies and dampings (dashed line); (3) chemical prior knowledge on multiplet structures as defined in the text (dash-dotted line). The marks correspond to the estimated R^{-1} values of ATP multiplets.

5. APPLICATION

To illustrate our theoretical study, we used quantitation results of *in vivo* ^{31}P signals of a rat brain. The measurements were performed on a nonanesthetized, but immobilized, Wistar rat at 2 T. Each signal was made up of 1000 averages and was acquired in 14 min. Methylene diphosphonic acid (MDPA) was used as an external reference. Signal quantitation was performed using the advanced time domain signal processing package MRUI, which provides facilities for supplying prior knowledge (35, 36). The VARPRO method based on a nonlinear least-squares algorithm was selected and the following

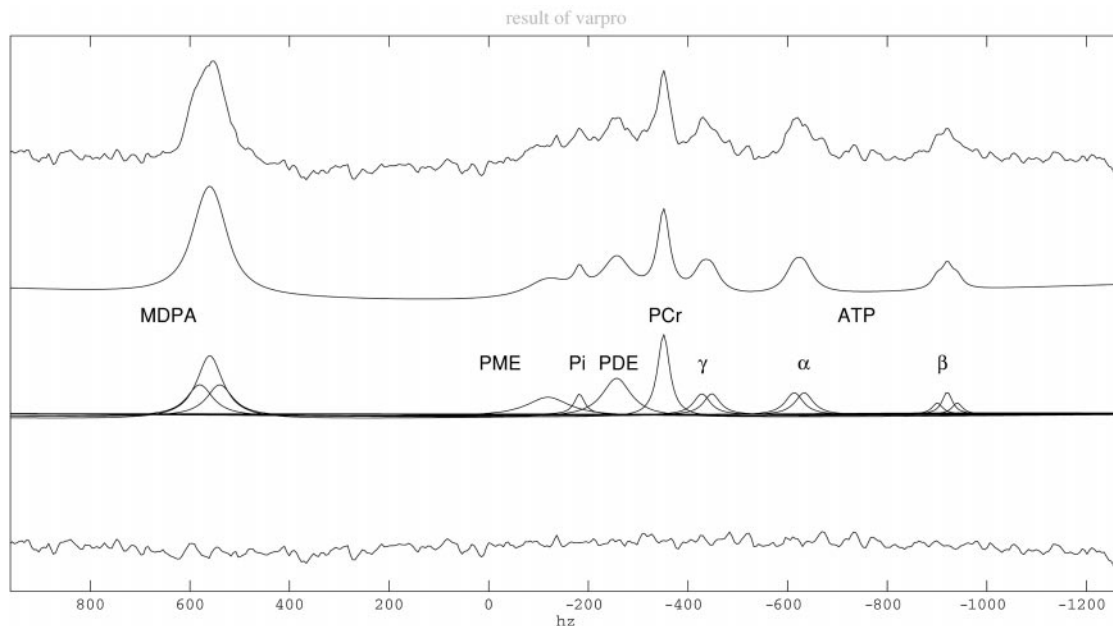


FIG. 5. *In vivo* ^{31}P spectra of a rat brain obtained at 2 T. MDPA was used as an external reference. The quantitation was done with VARPRO. The symmetric doublet structure for the γATP and αATP and the symmetric triplet structure for the βATP and MDPA were imposed. All scalar couplings were put equal to $J = 20$ Hz. From bottom to top: the experimental spectrum obtained after FFT of the acquired signal, the reconstructed spectrum obtained after FFT of the estimated signal, the spectrum of individual estimated peaks, and then the residue.

prior knowledge was imposed: (1) the ratios between the amplitudes of the peaks were 1:1 for the ATP doublets and 1:2:1 for the ATP and MDPA triplets, assuming that the weak scalar coupling approximation is valid. (2) The damping factors of the peaks within a multiplet were kept equal. (3) The phases of all peaks were set to 0 relative to the estimated zero-order phase and the dead time of the receiver was estimated. (4) All scalar couplings were put equal to 20 Hz. The Fourier transforms of the measured and fitted signals are shown in Fig. 5. Overlap factors were obtained from a previous quantitation result (37), enabling calculation of the reduction of the CRBs. The invoked prior knowledge increases the precision by an order of magnitude (see Fig. 4).

By considering pairs of peaks (e.g., the “doublet” formed by the PCr peak and the left peak of the γATP), the interaction terms corr_{c_1} , corr_{c_2} , and corr_{ω} between the peaks were computed from Eqs. [18] and [21] (see Table 4). When the interaction terms are near unity, the two peaks can be considered isolated. It is clear that the γ - and αATP doublets, the βATP triplet, and the MDPA triplet can be considered isolated structures. On the other hand, the peaks of the cluster inorganic phosphate, phosphomonoester, and phosphodiester strongly interfere with one another. Note that phosphocreatine and phosphodiester only slightly interfere.

Estimation of the ATP doublet and triplet model parameters severely suffer from *intramultiplet* overlap. As a result, corr_c and corr_{ω} reach very high values (see Fig. 3), e.g., for the αATP peaks the interaction terms are around $\text{corr}_c = 7$ and $\text{corr}_{\omega} = 3$.

Finally, note that a pairwise analysis as shown in Table 4 provides insight into interaction between the various structures present in a spectrum. In other words, our approach allows handling of measurements comprising many peaks.

6. CONCLUSIONS

We have derived analytical expressions for the asymptotic CRBs on the model parameters of a singlet, a doublet, and a

TABLE 4
Pairwise Analysis of an *in Vivo* ^{31}P Spectrum of a Rat Brain

Pair	R	corr_{c_1}	corr_{c_2}	corr_{ω}
MDPA-PME	0.07	1.01	1.01	1.00
PME-Pi	0.96	3.02	3.17	1.88
PME-PDE	0.62	1.72	1.66	1.32
PME-PCr	0.16	1.04	1.04	1.02
PME- γATP_1	0.11	1.02	1.02	1.01
Pi-PDE	0.88	2.23	1.99	1.52
Pi-PCr	0.15	1.04	1.04	1.02
Pi- γATP_1	0.10	1.02	1.02	1.01
PDE-PCr	0.57	1.29	1.34	1.16
PDE- γATP_1	0.30	1.10	1.10	1.05
PCr- γATP_1	0.21	1.09	1.09	1.05
γATP_1 - γATP_2	1.06	3.85	3.85	2.13
αATP_1 - αATP_2	1.43	6.85	6.85	3.04

Note. The interaction terms corr_{c_1} and corr_{c_2} , pertain respectively, to the left and the right peaks of the considered pairs.

triplet assuming exponential damping. These expressions are valid if a sufficiently large number of samples is used. This was done with and without prior knowledge. The following conclusions are drawn from these expressions:

1. The CRB of a parameter of a doublet peak is the product of the CRB for the same, but isolated, peak and an interaction term.
2. The interaction term provides valuable insight into the effects of overlap. For example, it depends only on the dampings and doublet splitting, but *not* on the amplitudes.
3. Conclusions (1) and (2) apply also for a triplet.
4. Imposition of prior knowledge does not modify conclusions (1) and (2). For overlapping peaks, the error reduction can be by an *order of magnitude*.
5. The results enable analysis of more complicated spectra.

ACKNOWLEDGMENTS

This work is supported by the EU programme "Training and Mobility of Researchers, Networks," Project FMRX-CT97-0160, and the Stichting voor Technische Wetenschappen (STW), Project DTN99.1683. The authors acknowledge fruitful discussions with R. de Beer, B. Fenet, H. Saint-Jalmes, and B. P. O. van Tongeren.

REFERENCES

1. C. R. Rao, Minimum variance and the estimation of several parameters, *Proc. Cambridge Phil. Soc.* **43**, 280–283 (1946).
2. H. Cramer, "Mathematical Methods of Statistics," University Press, Princeton (1946).
3. B. Levine, "Fondements Théoriques de la Radiotechnique Statistique," Edition Mir (1979).
4. H. Barkhuijsen, R. de Beer, and D. van Ormondt, Error theory for time-domain signal analysis with linear prediction and singular value decomposition, *J. Magn. Reson.* **67**, 371–375 (1986).
5. T. J. A. Jones, P. Hodgkinson, A. L. Barker, and P. J. Hore, Optimal sampling strategies for the measurement of spin-spin relaxation times, *J. Magn. Reson. B* **113**, 25–34 (1996).
6. C. E. Fursman and P. J. Hore, Distance determination in spin-correlated radical pairs in photosynthetic reaction centres by electron spin echo envelope modulation, *Chem. Phys. Lett.* **303**, 593–600 (1999).
7. Y. T. Zhang, H. N. Yeung, M. O'Donnell, and P. L. Carson, Determination of sample time for T1 measurement, *J. Magn. Reson. Imaging* **8**, 675–681 (1998).
8. P. Stoica and A. Nehorai, MUSIC, Maximum Likelihood, and Cramer-Rao bound, *IEEE Trans. Acoust. Speech Signal Processing* **37**(5), 720–741 (1989).
9. P. Stoica and A. Nehorai, MUSIC, Maximum Likelihood, and Cramer-Rao bound: Further results and comparisons, *IEEE Trans. Acoust. Speech Signal Processing* **38**(12), 2140–2150 (1990).
10. B. Hochwald and A. Nehorai, Concentrated Cramer-Rao bound expressions, *IEEE Trans. Inform. Theory* **40**(2), 363–371 (1994).
11. D. N. Swingler, Frequency estimation for closely spaced sinusoids: Simple approximations to the Cramer-Rao Lower Bound, *IEEE Trans. Signal Processing* **41**(1), 489–495 (1993).
12. H. B. Lee, The Cramer-Rao Bound on frequency estimates of signals closely spaced in frequency, *IEEE Trans. Signal Processing* **40**(6), 1508–1517 (1992).
13. S. F. Yau and Y. Bresler, A compact Cramer-Rao Bound expression for parametric estimation of superimposed signals, *IEEE Trans. Signal Processing* **40**(5), 1226–1230 (1992).
14. T. L. Marzetta, A simple derivation of the constrained multiple parameter Cramer-Rao Bound, *IEEE Trans. Signal Processing* **41**(6), 2247–2249 (1993).
15. T. Wigren and A. Nehorai, Asymptotic Cramer-Rao bounds for estimation of the parameters of damped sine waves in noise, *IEEE Trans. Signal Processing* **39**(4), 1017–1020 (1991).
16. C. Huegen, "The Influence of Prior Knowledge on Cramer-Rao Lower Bounds," Master's thesis, in Dutch, TU Delft (1993).
17. D. N. Swingler, Approximations to the Cramer-Rao lower bound for a single damped exponential signal, *Signal Processing* **75**(2), 197–200 (1999).
18. A. Macovski and D. Spielman, *In vivo* spectroscopic magnetic resonance imaging using estimation theory, *Magn. Reson. Med.* **3**, 97–104 (1986).
19. Waterloo Maple Incorporation, Maple v release 4, Copyright 1981–1996.
20. A. van den Bos, A Cramer-Rao Lower Bound for complex parameters, *IEEE Trans. Signal Processing* **42**(10), 2859 (1994).
21. A. van den Bos, "Handbook of Measurement Science," Wiley, New York (1982).
22. R. de Beer and D. van Ormondt, Analysis of NMR data using time domain fitting, in "NMR Basic Principles and Progress" (P. Diehl, E. Fluck, H. Gunther, R. Kosfeld, and J. Seeling, Eds.), pp. 202–248, Springer-Verlag, Berlin (1992).
23. E. O. Brigham, "The Fast Fourier Transform," Prentice-Hall, Englewood Cliffs, NJ (1974).
24. I. S. Gradshteyn and I. M. Ryzhik, "Table of Integrals, Series and Products," Academic Press, San Diego (1980).
25. J. Dupraz, "Théorie du Signal et Transmission de l'Information," Eyrolles, Paris (1989).
26. M. A. Delsuc and J. Y. Lallemand, Improvement of dynamic range in NMR by oversampling, *J. Magn. Reson.* **69**, 504–507 (1986).
27. S. Cavassila, "Méthodes de Traitement du Signal Appliquées à la Spectroscopie et à l'Imagerie par Résonance Magnétique," PhD thesis, Université Claude Bernard Lyon I (1996).
28. G. H. Golub and V. Pereyra, The differentiation of pseudo-inverses and non-linear least-squares problems whose variables separate, *SIAM J. Numer. Anal.* **10**, 413–432 (1973).
29. J. W. C. van der Veen, R. de Beer, P. R. Luyten, and D. van Ormondt, Accurate quantification of *in vivo* ³¹P NMR signals using the variable projection method and prior knowledge, *Magn. Res. Med.* **6**, 92–98 (1988).
30. L. Vanhamme, A. van den Boogaart, and S. Van Huffel, Improved method for accurate and efficient quantification of MRS data with use of prior knowledge, *J. Magn. Reson.* **129**, 35–43 (1997).
31. H. Chen, S. Van Huffel, D. van Ormondt, and R. de Beer, Parameter estimation with prior knowledge of known signal poles for the quantitation of NMR data in the time domain. *J. Magn. Reson. A* **119**(2), 225 (1996).
32. H. Chen, S. Van Huffel, and J. Vandewalle, Improved methods for exponential parameter estimation in the presence of known

- poles and noise, *IEEE Trans. Signal Processing* **45**, 1390–1393 (1997).
33. I. Dologlou and S. Van Huffel, Improved exponential data modeling with frequency prior-knowledge, *in* 4th International Conference on Mathematics in Signal Processing, Warwick, UK (1996).
 34. H. Chen, S. Van Huffel, A. Vandenboom, and P. J. Vandenbosch, Subspace-based parameter estimation of exponentially damped sinusoids using prior knowledge of frequency and phase, *Signal Processing* **59**, 129–136 (1997).
 35. A. van den Boogaart, S. Cavassila, L. Vanhamme, J. Totz, and P. Van Hecke, A complete software package for MR signal processing, *18th Ann. Int. Conf. IEEE Eng. Med. Biol. Soc.*, Amsterdam (1996).
 36. A. van den Boogaart, "MRUI Manual v96.3; A User's Guide to the Magnetic Resonance User Interface Software Package," ISBN: 90-9010509-3, TU Delft (1997).
 37. S. Cavassila, S. Deval, C. Huegen, D. van Ormondt, and D. Graveron-Demilly, The beneficial influence of prior knowledge on the quantitation of *in vivo* magnetic resonance spectroscopy signals. *Invest. Radiol.* **34**, 242–246 (1998).